ISSN 1070-3632, Russian Journal of General Chemistry, 2022, Vol. 92, No. 7, pp. 1262–1270. © Pleiades Publishing, Ltd., 2022.
Russian Text © The Author(s), 2022, published in Zhurnal Obshchei Khimii, 2022, Vol. 92, No. 7, pp. 1099–1108.

In Memory of V.I. Galkin

Interaction of Bovine Serum Albumin with Cationic Imidazolium Surfactants Containing a Methoxyphenyl Fragment

D. A. Kuznetsova[a],*, D. M. Kuznetsov[a], V. M. Zakharov[b], and L. Ya. Zakharova[a]

[a] *Arbuzov Institute of Organic and Physical Chemistry, Federal Research Center "Kazan Scientific Center of the Russian Academy of Sciences", Kazan, 420088 Russia*
[b] *Kazan National Research Technological University, Kazan, 420015 Russia*
**e-mail: Dashyna111@mail.ru*

Received March 31, 2022; revised May 5, 2022; accepted May 10, 2022

Abstract—Complexation ability of the imidazolium surfactants with a methoxyphenyl fragment towards a model protein, bovine serum albumin, has been investigated by means of physico-chemical methods (tensiometry, fluorescence spectroscopy, and dynamic as well as electrophoretic light scattering). The addition of bovine serum albumin has led to a decrease in the aggregation threshold of surfactants by 1.5–2 times. The imidazolium surfactants have formed stable complexes with the protein. The components binding has occurred primarily via the tyrosine amino acid fragments, involving hydrogen bonding and van der Waals interactions. Additional contribution of electrostatic forces and hydrophobic effect in the surfactant–albumin system has been revealed by means of dynamic and electrophoretic light scattering.

Keywords: cationic surfactants, bovine serum albumin, surfactant–protein complexes

DOI: 10.1134/S1070363222070143

Owing to the amphiphilic nature, surfactants have been widely applied in many high-performance technologies. In particular, they have been used to enhance solubility of hydrophobic compounds [1–3], development of nucleic acid carriers [4–6], modification of lipid carriers [7], and formation of the surfactant–protein complexes [8–9]. Since proteins are involved in many important biological processes, study of the interaction of cationic surfactant with proteins has attracted research interest [10]. Addition of a protein to a surfactant solution can significantly change the properties of the adsorption layer at the liquid/gas interface. In their turn, amphiphilic compounds can significantly affect the conformation state of proteins [11]. Bovine serum albumin (BSA) is among the best studied proteins widely used in practice. Its structure and physico-chemical properties have been well established; it consists of 583 amino acid residues, contains 17 disulfide bonds, and is negatively charged at neutral pH (isoelectric point 4.7). Structure of this water-soluble protein is very similar to that of human serum albumin (HSA) [12, 13]. It has been shown that, depending on the amphiphile structure, the binding of surfactant with BSA can occur via several mechanisms: electrostatic binding, hydrophobic interaction, hydrogen bonding, and π–π-stacking interaction (with aromatic fragments of the protein) [14–17]. However, despite numerous reports on the protein interaction with surfactants, further research in this field is important, since the relationships governing the complex formation efficiency in such systems have not been solidly established.

We have previously shown that monomeric amphiphiles bearing the imidazolium head group stabilize protein structures [18–20], whereas ammonium surfactant can lead to protein denaturation [21–22]. Such behavior has been explained by the ability of imidazolium surfactant to be involved in additional π–π-stacking interactions with tryptophan residues of BSA, which enhances the

Scheme 1.

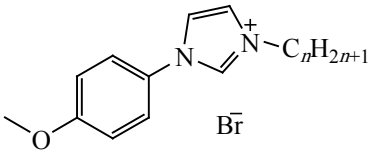

1

n = 10, 12, 14, 16.

complexes stability. In this study, we continued the investigation of the interaction between imidazolium amphiphiles and BSA using imidazolium surfactants bearing a methoxyphenyl fragment (**1**, n = 10, 12, 14, 16) as the example. The choice of the amphiphiles was due to the fact that biocompatible surfactants containing different natural fragments (pyrimidine, amino acid residues, or imidazolium) in the head group were promising building blocks for the formation of various types of nanocontainers [23–25]. Such surfactants ensure extended range of intermolecular and complementary interactions during self-assembly, thus combining high efficiency and low toxicity. Imidazolium surfactants are attractive due to the presence the imidazolium ring. This ring is found in histidine and can provide additional π–π-stacking interactions in the systems. Therefore, the presence of imidazolium ring is very important from the viewpoint of biology [26]. The presence of the methoxyphenyl is important in this regard as well. The compounds bearing a methoxyphenyl fragment are inhibitors of tubulin protein, which exhibit strong cytotoxic activity and prevent cancer cells mitosis [27–29]. It has been shown that the introduction of the methoxyphenyl fragment in the structure of imidazolium surfactants enhances antimicrobial activity and cytotoxic action of the amphiphiles [30]. Moreover, the presence of the methoxyphenyl fragment on the surfactant head group can alter the geometry of the amphiphilic with regard to the packing during aggregation, thus suggesting unusual binding mechanism during the surfactant–BSA complex formation. The experiments were performed at constant protein concentration (0.05 wt %) and varied concentration of the amphiphiles. The concentration choice was due to the synergetic effect observed at such concentration during the components interactions [19]. Structures of the considered surfactants are given in Scheme 1.

Aggregation properties of the surfactant–BSA systems were estimated by means of tensiometry (Fig. 1). Surface tension of the binary surfactant–protein systems was lower than for the individual surfactant systems, likely due to surface activity of BSA [31]. In the case of individual surfactants, the dependences of the surface tension on the amphiphiles concentration contained a single inflection point. Extension of the alkyl fragment by two carbon atoms led to the decrease in the critical micellization concentration (CMC) by approximately 2.5–3.5 times. The CMC values for individual surfactants **1** were as follows: 6.8 (n = 10), 2.6 (n = 12), 0.95 (n = 14), and 0.35 mM. (n = 16) [30]. For the binary systems surfactant **1**–BSA, the corresponding surface tension isotherms contained two inflection points. The first one, at low surfactant concentration (CAC_1) reflected the saturation of the interface with the amphiphile molecules attached to the protein macromolecule chain; formation of the surfactant–protein complexes began at that concentration. The second inflection point at high surfactant concentration, could correspond, as in the case of conventional polymer–surfactant complexes, to the saturation of the protein macromolecules with surfactant and the onset of the formation of free surfactant micelles (CAC_2) [6, 32]. The data on the aggregation threshold for surfactant **1** and surfactant **1**–BSA systems are combined in Table S1 (cf. Supplementary Information). It is to be seen that the formation of mixed surfactant–BSA aggregates began at the concentration 1.5–2 times lower than that for the individual surfactant aggregates.

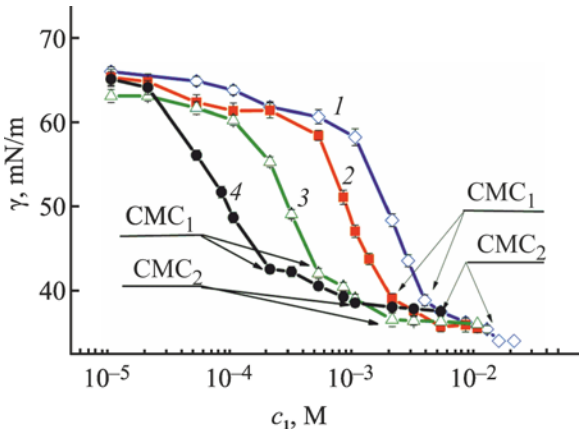

Fig. 1. Surface tension isotherms for the surfactant **1**–BSA binary mixtures with n = 10 (*1*), 12 (*2*), 14 (*3*), and 16 (*4*) at constant BSA concentration (0.05 wt%) at 25°C.

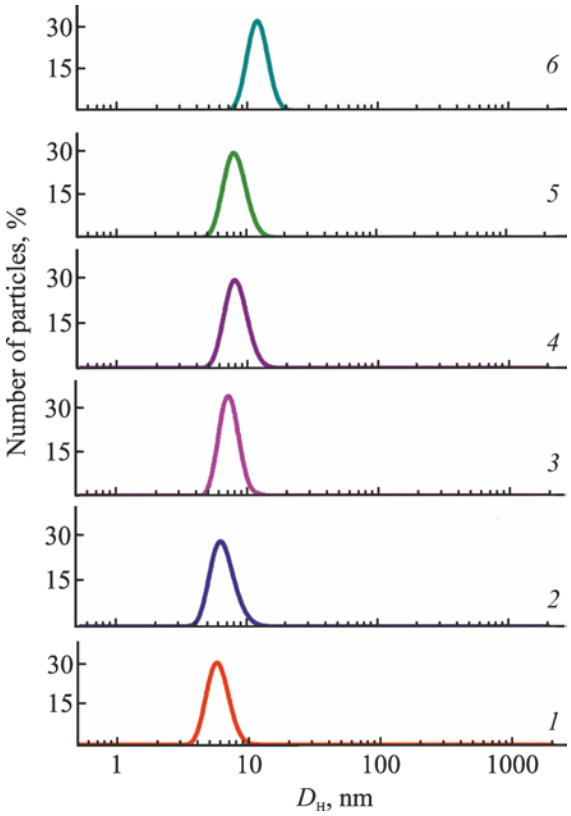

Fig. 2. Number-average size distribution of the aggregates for aqueous solutions of surfactant **1** (n = 10)–BSA at 25°C and surfactant concentration: 0 (*1*, BSA content 0.05 wt%), 0.01 (*2*), 0.1 (*3*), 1 (*4*), 5 (*5*), and 10 mM. (*6*).

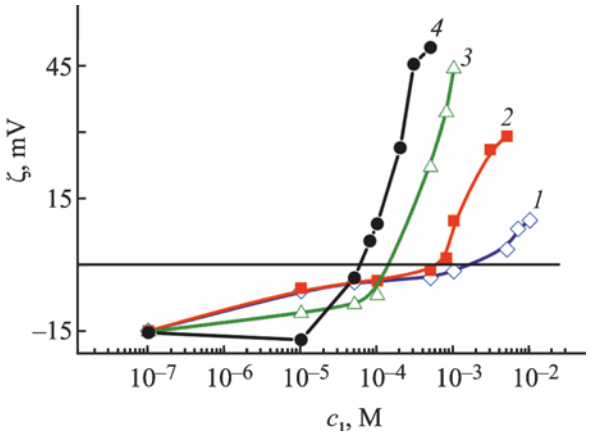

Fig. 3. Electrokinetic potential of the surfactant **1**–BSA binary mixtures with n = 10 (*1*), 12 (*2*), 14 (*3*), and 16 (*4*) as function of the surfactant concentration at 25°C.

Size of the complexes formed in the surfactant **1**–BSA binary systems was determined by means of dynamic light scattering (Figs. 2 and S1). It was revealed that the size of individual BSA aggregates was of 6–7 nm. Addition of different concentrations of the surfactants did not significantly affect the polypeptide size, the size of the surfactant **1**–BSA complexes being of 6–9 nm. The insignificant increase in the size of the complexes was observed only in the surfactant **1** (n =10)–BSA system at high concentration of the surfactant (10 mM). The size of the mixed aggregate under those conditions were of 10–12 nm. That fact could reflect partial denaturation of the protein molecule. It should be noted that small micelle-like aggregates with hydrodynamic diameter 2–4 nm were formed in the sysmets containing individual higher surfactant homologs at their concentration above CMC. In the case of **1** (n =10), larger aggregates with hydrodynamic diameter of 40–100 nm were formed [30]. As an example, Fig. 2 displays the number-average size distribution of the aggregates in the surfactant **1** (n =10)–BSA aqueous solutions.

Charge parameters of the surfactant **1**–BSA systems were assessed by means of electrophoretic light scattering (Fig. 3). BSA macromolecules were negatively charged, therefore it was expected that the addition of cationic surfactants would be accompanied by electrostatic binding of the components. That suggestion was confirmed by the experimental data showing the increase in the zeta potential and the change in its sign from negative to positive with the increase in the surfactant concentration in the considered systems. Increase in the length of the hydrocarbon fragment led to the decrease in its concentration corresponding to isoelectric point. That fact likely evidenced significant contribution of hydrophobic interaction in the complexes formation.

Efficiency of the surfactant **1** interaction with BSA was further assessed using different fluorescence methods. BSA contained three aromatic amino acids which could contribute into the protein fluorescence: tyrosine (Tyr), tryptophane (Trp), and phenylalanine (Phe). The contribution of Phe to emission is usually considered negligible due to low quantum yield [33]. Therefore, it could be considered that fluorescent properties of the protein were determined by tyrosine and tryptophane residues. Individual solution of BSA exhibited strong fluorescence peak at 340 nm. the recorded fluorescence spectra of the complexes revealed that the addition of the surfactants to BSA led to the fluorescence quenching

and bathochromic (red) shift of the maximum of the emission band (Figs. 4 and S2). Fluorescence quenching is usually due to the components binding. However, bathochromic shift is not typical of the interaction between cationic surfactants with BSA. Hyprsochromic shift usually accompanies the mixed complexes formation [18–20, 31]. However, it has been shown in [34] that bathochromic shift of the emission maximum with weakening of the BSA fluorescence points at the change of the microenvironment of the tryptophane residues, which can be caused by the increase in the medium micropolarity. Moreover, we observed the isosbestic points which can evidence the existence of bound and free surfactant in equilibrium [35–36]. Wavelengths of the isosbestic points were as follows: 376 nm for surfactant **1** (n =10)–BSA, 374 nm for surfactant **1** (n =12)–BSA, 367 for surfactant **1** (n =14)–BSA, and 364 nm for surfactant **1** (n =16)–BSA. It should be noted that the equilibrium was achieved at higher concentration of the surfactant for the amphiphiles with shorter hydrocarbon fragment. That fact could indirectly evidence the contribution of hydrophobic interactions to the complexes formation. As an example, Fig. 4 displays emission spectra of fluorescence for the surfactant **1** (n =10)–BSA binary system.

A series of quantitative parameters of the interaction in the surfactant **1**–BSA systems could be obtained from the fluorescence data. In detail, we graphically determined the Stern–Volmer coefficients at different temperatures using the Stern–Volmer equation (1) [37]:

$$\frac{F_0}{F} = 1 + K_{SV}[Q] = 1 + k_q \cdot \tau_0 [Q], \quad (1)$$

with F_0 being the fluorescence intensity in the absence of the quencher, F being the fluorescence intensity in the presence of certain concentration of the quencher, K_{SV} being the Stern–Volmer constant, [Q] being the quencher (surfactant) concentration, k_q being the bimolecular rate constant of the quenching, and τ_0 being average lifetime of the fluorophore (BSA) in the excited state, which equaled 10^{-8} s [37].

Using the Stern–Volmer constant, the bimolecular rate constant of quenching (k_q) could be determined, which allowed the conclusion on the predominant quenching mechanism in the considered systems. The fluorescence quenching is usually divided into dynamic and static quenching depending on the mechanism. Bimolecular

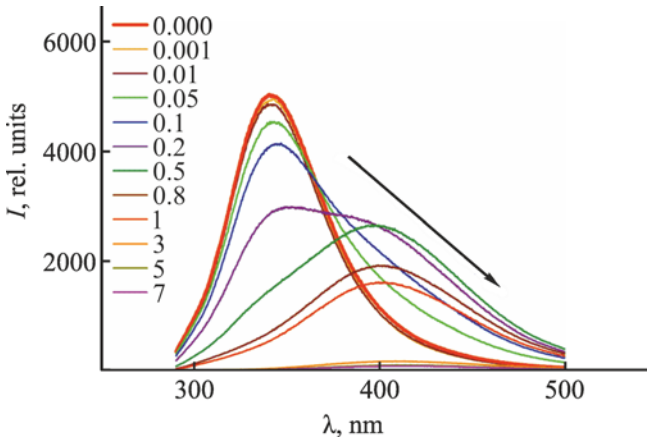

Fig. 4. Emission spectra of fluorescence of the surfactant **1** (n = 10)–BSA binary system with varied surfactant concentration (mM) and BSA content 0.05 wt %.

rate constant of quenching could be calculated using Eq. (2) [37]:

$$k_q = K_{SV}/\tau_0. \quad (2)$$

For instance, if the k_q is below 2×10^{10} L mol^{-1} s^{-1}, dynamic quenching predominates, and if the value is higher than 2×10^{10} L mol^{-1} s^{-1}, the quenching is static. The data for different temperatures are collected in Table 1. It is to be seen that the K_{SV} values for the considered systems were decreased with the increase in temperature. Furthermore, the calculated k_q values were 1–2 orders of magnitude higher that the maximum rate constant of quenching during collision-induced dynamic quenching (2×10^{10} L mol^{-1} s^{-1}). Those facts evidenced static quenching mechanism during formation of the surfactant **1**–BSA complexes, most likely suggesting that the surfactant and BSA formed noncovalently bound complex due to the surfactant molecules adsorption at hydrophobic domains of the protein [17].

Binding constants of the surfactants with BSA (K_a), numbers of the components binding sites (N), and thermodynamic parameters of the studied systems from the primary fluorescence data were calculated using Eqs. (3)–(5) [38]:

$$\log\frac{F_0 - F}{F} = \log K_a + N\log[Q], \quad (3)$$

$$\ln K_a = -\frac{\Delta H}{RT} + \frac{\Delta S}{R}, \quad (4)$$

$$\Delta G^\circ = \Delta H^\circ - T\Delta S^\circ, \quad (5)$$

Table 1. The values of the Stern–Volmer constant K_{SV}, constant of the components binding K_a, bimolecular rate constants of quenching K_q, and the number of binding sites of BSA and the surfactant N, and changes of enthalpy $\Delta H°$, entropy $\Delta S°$, and free Gibbs energy $\Delta G°$ for the studied systems at different temperatures

Surfactant **1**–BSA	T, K	$K_{SV}\times10^3$, L/mol	$K_a\times10^3$, L/mol	$K_q\times10^{10}$, L mol^{-1} s^{-1}	N	$\Delta H°$, kJ/mol	$\Delta S°$, J mol^{-1} K^{-1}	$\Delta G°$, kJ/mol
n = 10	298	9.8	8.70	98	1	–141.38	–397.41	–22.95
	303	5.7	6.30	57.4	1			–20.97
	308	4.3	1.10	43.1	0.8			–18.99
	313	3.8	0.76	37.8	0.76			–16.99
n = 12	298	6.3	15.85	62.6	1	–80.95	–191.22	–23.97
	303	6.4	7.94	63.8	1			–23.01
	308	6.5	5.49	64.6	1			–22.05
	313	6.4	5.01	63.8	1			–21.10
n = 14	298	13.5	15.85	135.3	1	–41.8	–59.3	–24.1
	303	12.0	15.14	119.2	1			–23.8
	308	11.9	8.13	119.0	1			–23.5
	313	10.8	7.94	108.2	1			–23.2
n = 16	298	15.5	1023.29	155.3	1.2	–51.43	–56.2	–34.6
	303	14.9	870.96	149.2	1.4			–34.3
	308	13.9	794.33	139.9	1.4			–34.0
	313	11.7	346.74	117.5	1.6			–33.7

with $\Delta H°$ being the change of the system enthalpy, $\Delta S°$ being the change of the system entropy, R being universal gas constant (8.314 J mol^{-1} K^{-1}), T being the experiment temperature, and $\Delta G°$ being the change of the system Gibbs free energy. The data are collected in Table 1. The obtained results revealed that the increase in temperature led to the decrease in the binding constant in the considered systems, reflecting the decrease in the complexes stability [12]. However, it should be noted that sufficiently strong binding between the components was achieved, which was strengthened with the increase in the length of the hydrocarbon part of the surfactant. The values of N for the surfactant **1**–BSA complexes were about unity, evidencing a single binding site in BSA available for the interaction with the surfactant. The values of the change in enthalpy $\Delta H°$, entropy $\Delta S°$, and Gibbs free energy $\Delta G°$ during the surfactant–BSA complexes formation were obtained from the values of the binding constant K_a [Eqs. (3)–(5), Table 1]. It is known that certain intermolecular interactions are predominant in the complexes formation depending on the change in the thermodynamic functions $\Delta H°$ and $\Delta S°$ [38]: (1) hydrogen bonding and van der Waals interactions at $\Delta H° < 0$ and $\Delta S° < 0$, (2) hydrophobic interactions at $\Delta H° > 0$ and $\Delta S° > 0$, and (3) electrostatic interactions at $\Delta H° < 0$ and $\Delta S° > 0$.

According to the obtained data, hydrogen bonding and van der Waals interactions were predominant during the formation of the surfactant **1**–BSA complexes. The oxygen and nitrogen atoms of the surfactants, bearing lone-electron pair, could be involved in the hydrogen bond formation, the proton donors being carboxylic and (to a lesser extent) hydroxyl groups of the amino acid residues. Negative values of the Gibbs free energy of the interaction evidenced thermodynamic favorability of the surfactant–BSA complex formation.

UV-visible absorption spectroscopy is a simple and available method to investigate the formation of the surfactant–protein complexes. In contrast to fluorescence spectroscopy reflecting the electronic transitions from the excited state to the ground one, the absorption spectroscopy probes the reverse transitions. Measurement of UV absorption at 280 nm is used to investigate the proteins containing tyrosine (Tyr) and tryptophane (Trp) units. The absorption in the said range is due to the n–π^* transitions in Tyr and Trp [39]. Therefore, the influence of different amounts of the surfactants on the BSA structural changes were investigated by measuring the absorption

spectra using the surfactant **1** (n = 16)–BSA system as example (Fig. 5). It is to be seen that the addition of surfactant **1** (n = 16) to BSA and the increase in the concentration of the surfactant in the system led to the increase in absorbance and significant hypsochromic shift. The observed change in the absorbance evidenced in favor of the static mechanism of BSA fluorescence quenching in the presence of the surfactant [40], since it is known that dynamic quenching affects only the excited state of the molecule and induces no change in the absorption spectra [41]. The obtained results coincided with the published data on the complex formation between the components in scope of the static quenching of fluorescence. The shift of the absorption maximum could be also attributed to the change in the microenvironment of the tyrosine and tryptophane units [40].

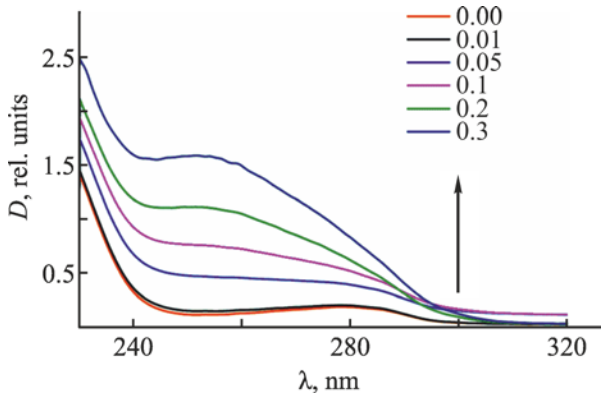

Fig. 5. Absorption spectra of BSA in the absence and in the presence of surfactant **1** (n = 16) at 25°C. BSA content 0.05 wt %. Surfactant concentration is given in mM.

To elucidate the amino acid residue (tyrosine or tryptophane) involved in the interaction with the surfactant molecules, we took advantage of synchronous fluorescence spectroscopy with constant wavelength difference Δλ : Δλ = 20 nm to detect the binding with the tyrosine unit and Δλ = 60 nm for the tryptophane unit (Figs. 6, S3).

From the data in Figs. 6 and S3 it is to be seen that addition of the surfactants to BSA led to the quenching of tyrosine and tryptophane fluorescence; for both fragments, bathochromic shift of the emission band maximum was observed. Hence, it could be concluded that the presence of the surfactant in solution led to the increase in the medium polarity about the tyrosine and tryptophane residues, the surfactant likely being efficiently bound with both fragments. Analysis of the fluorescence weakening upon the surfactant addition could be used to elucidate the fragment interacting stronger with compounds **1** [16]. For the considered surfactants, the fluorescence quenching at Δλ = 20 nm was stronger than at Δλ = 60 nm. That fact pointed at stronger interaction of the amphiphile molecules with the tyrosine units than with tryptophane ones. It is interesting to note that the non-functionalized

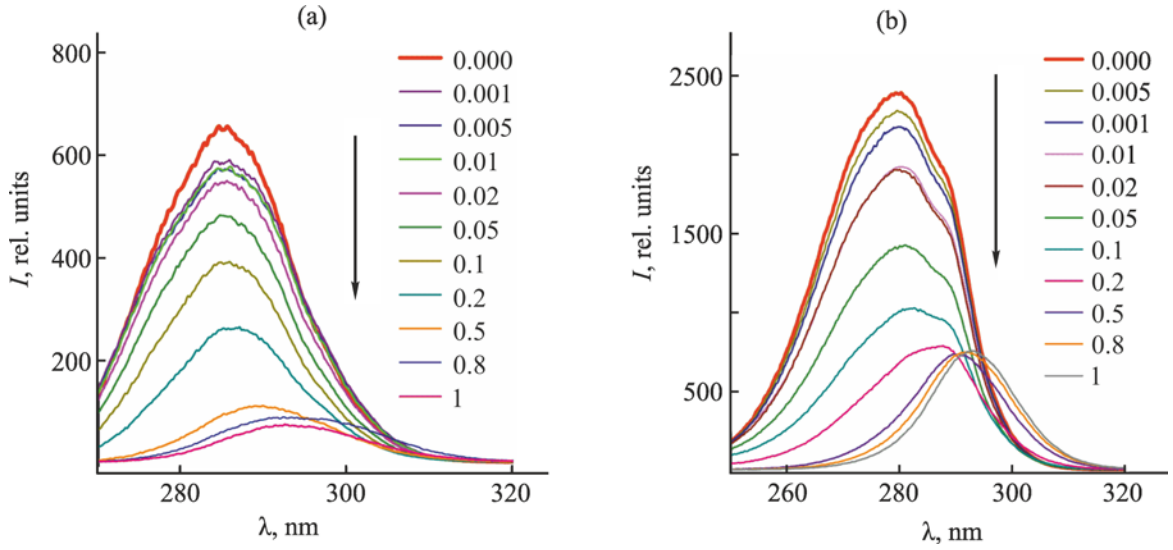

Fig. 6. Synchronous spectra of BSA fluorescence in the presence of different concentrations of surfactant (mM.) for the surfactant **1** (n = 14)–BSA binary system at 25°C. Δλ = 20 (a), 60 nm (b).

imidazolium surfactants have been predominantly bound to the protein at the tryptophane residues [18, 19].

In summary, the interaction of the amphiphiles containing the imidazolium head group and the methoxyphenyl fragment, differing in the hydrocarbon moiety length, with bovine serum albumin was studied using a set of physico-chemical methods. Formation of stable complexes with hydrodynamic diameter of 6–9 nm was demonstrated. The fluorescence spectroscopy data revealed that the components binding occurred via the tryptophane and tyrosine amino acid units, the binding at the tyrosine one being predominant. It is interesting to note that the amphiphiles binding with the protein occurred via the tryptophane (but not tyrosine) units in the case of the non-substituted imidazolium surfactant. It was found that hydrogen bonding and van der Waals interactions between the components were predominant mechanisms of the surfactant–BSA complexes formation. However, weaker contribution of electrostatic and hydrophobic interactions was confirmed by means of dynamic and electrophoretic light scattering. It should be noted that no significant difference in the formation of the surfactant–BSA complexes was observed with the variation of the hydrocarbon fragment length. Likely, the nature of the surfactant head group was the key factor determining the mechanisms of the complexes formation.

EXPERIMENTAL

The methoxyphenyl-containing imidazolium surfactants differing in the hydrocarbon moiety length were prepared via the reaction of 1-(4-methoxyphenyl) imidazole with the corresponding alkyl bromides in acetonitrile, followed by the target product purification in diethyl ether [30]. Bovine serum albumin (99%, Sigma-Aldrich) was used. Water purified using the Milli-Q system was used to prepare the surfactants and the protein solutions.

Surface tension of the solutions was determined using a Krűss K06 tensiometer (Germany) via the ring tear-off method. Fluorescence spectra of the surfactant–BSA binary mixtures were recorded using a Hitachi F-7100 spectrofluorimeter (Hitachi High-Tech Corporation, Japan) at temperature 25, 30, 35, and 40°C and excitation wavelength 280 nm. The emission spectra were recorded over the 290–450 nm range at scanning rate 1200 nm/min. The measurements were performed in 1 cm cell. Synchronous fluorescence spectra were recorded over the 200–500 nm range at scanning rate 1200 nm/min and two fixed differences between the excitation and emission wavelengths: $\Delta\lambda$ = 20 and 60 nm [42]. Size and zeta potential of the surfactant–BSA complexes were determined using a ZetaSizer Nano nanoparticles analyzer (Malvern, Great Britain). The measurements were performed at the scattering angle 173°. The obtained signals were processed via frequency-phase analysis of the scattering light using the Stokes–Einstein equation (6) for spherical particles:

$$D = kT/6\pi\eta R, \quad (6)$$

with k being the Boltzmann's constant, T being absolute temperature, η being the solvent viscosity, and R being hydrodynamic radius. Electrophoretic mobility of the particles in the samples was transformed in the zeta potential value using the Smoluchowski equation (7):

$$\zeta = \mu\eta/\varepsilon, \quad (7)$$

with ζ being zeta potential, η being dynamic viscosity of the liquid, μ being electrophoretic mobility of the particles, and ε being dielectric constant of the medium.

AUTHOR INFORMATION

D.A. Kuznetsova, ORCID: https://orcid.org/0000-0002-6981-4868

D.M. Kuznetsov, ORCID: https://orcid.org/0000-0002-9572-3708

V.M. Zakharov, ORCID: https://orcid.org/0000-0002-3982-2277

L.Ya. Zakharova, ORCID: https://orcid.org/0000-0002-2981-445X

FUNDING

This study was financially supported by the Russian Science Foundation (grant no. 21-73-00033).

CONFLICT OF INTEREST

No conflict of interest was declared by the authors.

SUPPLEMENTARY INFORMATION

The online version contains supplementary material available at https://doi.org/10.1134/S1070363222070143.

REFERENCES

1. Gaynanova, G.A., Valeeva, F.G., Kushnazarova, R.A., Bekmukhametova, A.M., Zakharov, S.V., Mirgoro-

dskaya, A.B., and Zakharova, L.Ya., *Russ. J. Phys. Chem. (A)*, 2018, vol. 92, no. 7, p. 1400. https://doi.org/10.1134/S0036024418070129

2. Lalthlengliani, J., Gurung, J., and Pulikkal, A.K., *J. Mol. Liq*., 2022, vol. 354, article 118823. https://doi.org/10.1016/j.molliq.2022.118823
3. Gabdrakhmanov, D.R., Samarkina, D.A., Krylova, E.S., Kapitanov, I.V., Karpichev, Y., Latypov, Sh.K., Semenov, V.E., Nizameev, I.R., Kadirov, M.K., and Zakharova, L.Ya., *J. Surfact. Deterg*., 2019, vol. 22, no. 4, p. 865. https://doi.org/10.1002/jsde.12257
4. St. John, P.M., Westervelt, K., Rimawi, A., and Kawakita, T., *Biophys. Chem*., 2022, vol. 281, article 106734. https://doi.org/10.1016/j.bpc.2021.106734
5. Gabdrakhmanov, D., Samarkina, D., Semenov, V., Syakaev, V., Giniyatullin, R., Gogoleva, N., and Zakharova, L., *Colloids Surf. (A)*, 2015, vol. 480, p. 113. https://doi.org/10.1016/j.colsurfa.2014.10.036
6. Kuznetsova, D.A., Gabdrakhmanov, D.R., Kuznetsov, D.M., Lukashenko, S.S., Zakharov, V.M., Sapunova, A.S., Amerhanova, S.K., Lyubina, A.P., Voloshina, A.D., Salakhieva, D.V., and Zakharova, L.Ya., *Molecules*, 2021, vol. 26, p. 2363. https://doi.org/10.3390/molecules26082363
7. Kuznetsova, D.A., Vasileva, L.A., Gaynanova, G.A., Pavlov, R.V., Sapunova, A.S., Voloshina, A.D., Sibgatullina, G.V., Samigullin, D.V., Petrov, K.A., Zakharova, L.Ya., and Sinyashin, O.G., *J. Mol. Liq*., 2021, vol. 330, article 115703. https://doi.org/10.1016/j.molliq.2021.115703
8. Ud din Parray, M., Maurya, N., Ahmad Wani, F., Borse, M.S., Arfin N, Malik, M.A., and Patel, R., *J. Mol. Struct*., 2019, vol. 1175, p. 49. https://doi.org/10.1016/j.molstruc.2018.07.078
9. Vlasova, I.M., Vlasov, A.A., Grapendaal, G.R., and Saletskii, A.M., *Russ. J. Phys. Chem. (A)*, 2018, vol. 92, no. 4, p. 714. https://doi.org/10.1134/s0036024418040325
10. Fatma, I., Sharma, V., Thakur, R.C., and Kumar, A., *J. Mol. Liq*., 2021, vol. 341, article 117344. https://doi.org/10.1016/j.molliq.2021.117344
11. Kuznetsov, D.M., Kuznetsova, D.A., Gabdrakhmanov, D.R., Lukashenko, S.S., Nikitin, Y.N., and Zakharova, L.Ya., *Surf. Innovations*, 2021, article 2100044. https://doi.org/10.1680/jsuin.21.00044
12. Shalaeva, Y.V., Morozova, J.E., Shumatbaeva, A.M., Nizameev, I.R., Kadirov, M.K., and Antipin, I.S., *J. Mol. Liq*., 2019, vol. 286, article 110879. https://doi.org/10.1016/j.molliq.2019.110879
13. Karush, F., *J. Am. Chem. Soc*., 1950, vol. 72, p. 2705. https://doi.org/10.1021/ja01162a099
14. Patel, R., Mir, M.U.H., Maurya, J.K., Singh, U.K., Maurya, N., Parray M. ud din, Khan, A.B., and Ali, A., *Luminescence*, 2015, vol. 3, p. 1233. https://doi.org/10.1002/bio.2886
15. Hoque, M.A., Ahmed, F., Halim, M.A., Molla, M.R., Rana, S., Rahman, M.A., and Rub, M.A., *J. Mol. Liq*., 2018, vol. 260, no. 15, p. 121. https://doi.org/10.1016/j.molliq.2018.03.069
16. Zhou, T., Ao, M., Xu, G., Liu, T., and Zhang, J., *J. Colloid Interface Sci*., 2013, vol. 389, p. 175. https://doi.org/10.1016/j.jcis.2012.08.067
17. Kuznetsova, D.A., Gabdrakhmanov, D.R., Lukashenko, S.S., Faizullin, D.A., Zuev, Y.F., Nizameev, I.R., Kadirov, M.K., Kuznetsov, D.M., and Zakharova, L.Ya., *J. Mol. Liq*., 2020, vol. 307, article 113001. https://doi.org/10.1016/j.molliq.2020.113001
18. Samarkina, D.A., Gabdrakhmanov, D.R., Lukashenko, S.S., Nizameev, I.R., Kadirov, M.K., and Zakharova, L.Ya., *J. Mol. Liq*., 2019, vol. 275, p. 232. https://doi.org/10.1016/j.molliq.2018.11.082
19. Samarkina, D.A., Gabdrakhmanov, D.R., Lukashenko, S.S., Khamatgalimov, A.R., and Zakharova, L.Ya., *Russ. J. Gen. Chem*., 2017, vol. 87, no. 12, p. 2826. https://doi.org/10.1134/S1070363217120118
20. Kuznetsova, D.A., Gabdrakhmanov, D.R., Lukashenko, S.S., Voloshina, A.D., Sapunova, A.S., Kashapov, R.R., and Zakharova, L.Ya., *Chem. Phys Lipids*, 2019, vol. 223, article 104791. https://doi.org/10.1016/j.chemphyslip.2019.104791
21. Misra, P.K., Dash, Um., and Maharan, S., *Colloids Surf. (A)*, 2015, vol. 483, p. 36. https://doi.org/10.1016/j.colsurfa.2015.06.052
22. Gabdrakhmanov, D.R., Valeeva, F.G., Samarkina, D.A., Lukashenko, S.S., Mirgorodskaya, A.B., and Zakharova, L.Ya., *Colloids Surf. (A)*, 2018, vol. 558, p. 463. https://doi.org/10.1016/j.colsurfa.2018.09.008
23. Joondan, N., Jhaumeer Laulloo, S., and Caumul, P., *J. Dispers. Sci. Technol*., 2018, vol. 39, p. 1550. https://doi.org/10.1080/01932691.2017.1421085
24. Kashapov, R., Gaynanova, G., Gabdrakhmanov, D., Kuznetsov, D., Pavlov, R., Petrov K, Zakharova, L., and Sinyashin, O., *Int. J. Mol. Sci*., 2020, vol. 21, p. 6961. https://doi.org/10.3390/ijms21186961
25. Gabdrakhmanov, D.R., Kuznetsova, D.A., Saifina, L.F., Shulaeva, M.M., Semenov, V.E., and Zakharova, L.Ya.,

Colloids Surf. (A), 2020, vol. 599, p. 124853. https://doi.org/10.1016/j.colsurfa.2020.124853

26. Kumar, H. and Kaur, G., *Front. Chem.*, 2021, vol. 9, p. 667941. https://doi.org/10.3389/fchem.2021.667941
27. Álvarez, R., Álvarez, C., Mollinedo, F., Sierra, B.G., Medarde, M., and Peláez, R., *Bioorg. Med. Chem.*, 2009, vol. 17, p. 6422. https://doi.org/10.1016/j.bmc.2009.07.012
28. Magalhães, H.I.F., Bezerra, D.P., Cavalcanti, B.C., Wilke, D.V., Rotta, R., Lima, D.P., Beatriz, A., Alves, A.P.N.N., Bitencourt, F.S., Figueiredo, I.S.T., Alencar, N.M.N., Costa-Lotufo, L.V., Moraes, M.O., and Pessoa, C., *Cancer Chemother. Pharmacol.*, 2011, vol. 68, p. 45. https://doi.org/10.1007/s00280-010-1446-2
29. Magalhães, H.I.F., Cavalcanti, B.C., Bezerra, D.P., Wilke, D.V., Paiva, J.C.G., Rotta, R., Lima, D.P., Beatriz, A., Burbano, R.R., Costa-Lotufo, L.V., Moraes, M.O., and Pessoa, C., *Toxicol. In Vitro*, 2011, vol. 25. P., 2048. https://doi.org/10.1016/j.tiv.2011.08.007
30. Kuznetsova, D.A., Kuznetsov, D.M., Amerhanova, S.K., Buzmakova, E.V., Lyubina, A.P., Syakaev, V.V., Nizameev, I.R., Kadirov, M.K., Voloshina, A.D., and Zakharova, L.Ya., *Langmuir*, 2022. https://doi.org/10.1021/acs.langmuir.2c00299
31. Mir, M.A., Khan, J.M., Khan, R.H., Rather, G.M., and Dar, A.A., *Colloids Surf. (B)*, 2010, vol. 77, p. 54. https://doi.org/10.1016/j.colsurfb.2010.01.005
32. Kuznetsova, D.A., Gabdrakhmanov, D.R., Kuznetsov, D.M., Lukashenko, S.S., and Zakharova, L.Ya., *Russ. J. Phys. Chem. (A)*, 2020, vol. 94, no. 11, p. 2337. https://doi.org/10.1134/S0036024420110199
33. Yin, T., Qin, M., and Shen, W., *Colloids Surf. (A)*, 2014, vol. 461, p. 22. https://doi.org/10.1016/j.colsurfa.2014.07.012
34. Ojha, B. and Das, G., *J. Phys. Chem. (B)*, 2010, vol. 114, p. 3979. https://doi.org/10.1021/jp907576r
35. He, W., Li, Y., Xue, C., Hu, Z., Chen, X., and Sheng, F., *Bioorg. Med. Chem.*, 2005, vol. 13, p. 1837. https://doi.org/10.1016/j.bmc.2004.11.038
36. Joondan, N., Laulloo, S.J., and Caumul, P., *J. Dispers. Sci. Technol.*, 2018, vol. 39, p. 1550. https://doi.org/10.1016/j.jphotochem.2006.06.015
37. Wang, Y., Jiang, X., and Zhou, L., *Colloids Surf. (A)*, 2013, vol. 436, p. 1159. https://doi.org/10.1016/j.colsurfa.2013.08.045
38. Suryawanshi, V.D., Walekar, L.S., Gore, A.H., Anbhule, P.V., and Kolekar, G.B., *J. Pharm. Anal.*, 2016, vol. 6, p. 56. https://doi.org/10.1016/j.jpha.2015.07.001
39. Li, Y. and Lee, J.S., *Anal. Chim. Acta*, 2019, vol. 1063, p. 18. https://doi.org/10.1016/j.aca.2019.02.024
40. Kaur, N., Kaur, G., Kaur, H., and Chaudhary, G.R., *J. Mol. Liq.*, 2022, vol. 345, p. 117818. https://doi.org/10.1016/j.molliq.2021.117818
41. Lala, H., Akrama, M., and Kabir-ud-Din, *Colloids Surf. (A)*, 2022, vol. 646, p. 128944. https://doi.org/10.1016/j.colsurfa.2022.128944
42. Singh, I., Luxami, V., and Paul, K., *Spectrochim. Acta (A)*, 2020, vol. 235, no. 5, p. 118289. https://doi.org/10.1016/j.saa.2020.118289